

## Structure-activity relationship of novel macrocyclic biased apelin receptor agonists

Alexandre Murza,<sup>a,c,‡</sup> Xavier Sainsily,<sup>a,c,‡</sup> Jérôme Côté,<sup>a,c</sup> Laurent Bruneau-Cossette,<sup>a,c</sup> Élie Besserer-Offroy,<sup>a,c</sup> Jean-Michel Longpré,<sup>a,c</sup> Richard Leduc,<sup>a,c</sup> Robert Dumaine,<sup>a</sup> Olivier Lesur,<sup>b,c</sup> Mannix Auger-Messier,<sup>b</sup> Philippe Sarret<sup>a,c,\$</sup> and Éric Marsault<sup>a,c,\$,\*</sup>

<sup>a</sup> Département de Pharmacologie et Physiologie, Faculté de Médecine et des Sciences de la Santé, Université de Sherbrooke, Sherbrooke (QC), J1H 5N4, Canada.

<sup>b</sup> Département de Médecine, Faculté de Médecine et des Sciences de la Santé, Université de Sherbrooke, Sherbrooke (QC), J1H 5N4, Canada.

<sup>c</sup> Institut de Pharmacologie de Sherbrooke, Université de Sherbrooke, Sherbrooke (QC), J1H 5N4, Canada.

<sup>‡</sup> These authors contributed equally to this work.

<sup>\$</sup> These authors contributed equally to directing this study.

### AUTHOR INFORMATION

#### Corresponding Author

\* Prof. Éric Marsault

Phone: +1 819.821.8000 ext 72433

Fax: +1 819.564.5400

Email: [eric.marsault@usherbrooke.ca](mailto:eric.marsault@usherbrooke.ca)

**Notes:** The authors declare no competing financial interest.

## Abstract

Apelin is the endogenous ligand for the G protein-coupled receptor APJ and exerts a key role in regulating cardiovascular function. We report here a novel series of macrocyclic analogues of apelin-13 where the C- and N-terminal exocyclic residues as well as the macrocycle composition were chemically-modified to explore the structure-activity relationships of these compounds on the APJ receptor. To this end, we investigated the binding properties of these analogues and monitored their ability to modulate the G-protein-dependent and G-protein-independent signalling pathways. In this series, the position and the aromatic properties of the C-terminal residue is a critical determinant for APJ interaction and  $\beta$ -arrestin recruitment, as previously demonstrated for linear apelin-13 derivatives. This study also led to the identification of compound **18** displaying an affinity in the micromolar range and a drastically simplified chemical structure, thus representing a promising starting point for further development of new macrocyclic analogues. We finally discovered compounds **4**, **11** and **15**, three potent G protein-biased apelin receptor agonists exhibiting affinity in the nanomolar range for APJ. These macrocyclic compounds represent very useful pharmacological tools to explore the therapeutic potential of the apelinergic system.

## Introduction

The apelin receptor (APJ, APLNR, or angiotensin receptor-like 1) is a member of the class A G-protein-coupled receptor (GPCR) superfamily and shares 31% sequence identity with the angiotensin II receptor type 1 (AT1R).<sup>1</sup> APJ was orphanized in 1998 when its endogenous ligand, apelin, was isolated from bovine stomach extracts.<sup>2</sup> Apelin is derived from a 77-amino acid precursor, pre-proapelin, which is converted into several isoforms of different lengths after proteolysis: apelin-36, -17, -13 (or its pyroglutamate analogue Pyr1-apelin-13),<sup>2-4</sup> the latter being the major form in circulation.<sup>5</sup> The apelinergic system has been detected in many peripheral tissues, such as the heart, kidney and pancreas, as well as in the central nervous system, especially the hypothalamus and spinal cord.<sup>3,6-8</sup> The apelin/APJ complex has been associated with diverse therapeutic indications, such as diabetes, obesity, gastrointestinal diseases, cancer and HIV infection.<sup>9,10</sup> However, the most notable and described role of the apelinergic system remains its association with the cardiovascular system homeostasis, where it exerts vascular and inotropic effects.<sup>11-14</sup> Indeed, intravenous administration of apelin-13 causes a lowering of mean arterial pressure (MAP) in rodents via a nitric oxide (NO)-dependent mechanism<sup>2,3,15</sup> as well as in healthy volunteers or patients exhibiting heart failure.<sup>16,17</sup> Activation of APJ triggers intracellular G-protein-dependent signalling pathways such as inhibition of forskolin-induced cAMP production,<sup>4,6</sup> and phosphorylation of extracellular signal-regulated kinases 1/2 (ERK1/2), Akt and p70S6K.<sup>18-20</sup> Upon activation, APJ also recruits both  $\beta$ -arrestin1 and  $\beta$ -arrestin2 and internalizes through different intracellular trafficking routes depending on the agonist.<sup>21</sup> Recently, a second endogenous ligand of APJ named ELABELA/Toddler was

discovered.<sup>22,23</sup> Similarly to apelin, ELABELA activates the  $G\alpha_{i/o}$ -dependent signalling pathways, recruits  $\beta$ -arrestins and efficiently modulates the cardiovascular system.<sup>24,25</sup> The conformation of apelin-17 in solution was elucidated by 2D NMR and circular dichroism, demonstrating no  $\alpha$ -helical or  $\beta$ -sheet secondary structure.<sup>26</sup> However, the Arg2-Pro3-Arg4-Leu5 moiety of apelin-13 was reported to adopt a more ordered structure. This hypothesis is further supported by molecular modeling studies<sup>27</sup> and alanine scan that pinpoint Arg2, Arg4 and Leu5 as key residues involved in binding to APJ and in  $G\alpha_{i/o}$ -dependent signalling.<sup>6</sup> The C-terminal Phe residue of apelin-13 also plays a critical role for APJ interaction and activation.<sup>6,28-31</sup> The structure-activity relationship (SAR) of apelin is the subject of a growing body of literature and was reviewed recently.<sup>32</sup> Of particular interest, the use of macrocyclic derivatives of the endogenous ligands of APJ appears to be a promising avenue to better probe the SAR of the apelin/APJ complex. Indeed, to interact with its target, the ligand has to adopt a bioactive conformation, which increases the entropic costs. If constrained in a binding conformation, the requisite rearrangement to bind to the target is lower, thus increasing affinity.<sup>33</sup> Thus, constraining the ligand via macrocyclization is a viable strategy for pre-organizing a binding conformation. Several groups have already exploited this strategy to design macrocyclic analogues of apelin-13 (**Figure 1**). The endocyclic position of the main pharmacophore of apelin-13, Arg2-Pro3-Arg4-Leu5, was explored and led to molecular modeling studies that suggest the presence of a  $\beta$ -turn.<sup>27</sup> This group also reported the discovery of a cyclic bivalent apelin receptor antagonist exhibiting an affinity of 93 nM based on Arg2-Pro3-Arg4-Leu5 moiety.<sup>34</sup> Likewise, using molecular dynamics simulations of apelin/APJ interactions, Brame and coworkers recently reported a macrocyclic analogue of apelin-13, MM07, where Cys

residues were incorporated to cyclize by a disulfide bridge the crucial pharmacophore mentioned above.<sup>35</sup> This macrocycle, described as a biased compound toward G-protein activation versus  $\beta$ -arrestins recruitment, caused a dose-dependent increase in cardiac output following intravenous administration to rats and raised forearm blood flow in healthy volunteers. A patent (US 2013/0196899 A1) also reports a series of bridged apelin-13 derivatives using a variety of linkers such as disulfides, esters and amides (**Figure 1**). In order to further investigate the SAR of the apelin-13/APJ system, we designed and synthesized a novel series of macrocyclic analogues of apelin-13 bridged with alkene functions. These compounds were assessed in binding affinity and a bioluminescence resonance energy transfer (BRET) assay was conducted from the activation of  $G\alpha_{i1}$  and  $G\alpha_{oA}$  subunits to the recruitment of  $\beta$ -arrestins1 and 2 in order to define their signalling profiles. Finally, the impact on blood pressure of selected macrocycles was evaluated.

Accepted Manuscript

## Results and Discussion

### Design and synthesis of macrocyclic analogues of apelin-13

Macrocycles were synthesized on solid phase using the Fmoc strategy as depicted in **Scheme 1**. Peptide elongation was carried out as described previously.<sup>30</sup> Briefly, the first Fmoc N-protected C-terminal amino acid was anchored to Wang resin (loading of 0.3 mmol/g) via a Mitsunobu reaction in the presence of triphenylphosphine (PPh<sub>3</sub>) and diisopropylazodicarboxylate (DIAD) in tetrahydrofuran (THF). Unreacted hydroxyl groups were capped with a mixture of DCM/MeOH/DIPEA (7/2/1). The Fmoc group was deprotected with a solution of piperidine/*N,N*-dimethylformamide (DMF, 1/5). The following Fmoc N-protected amino acids were then coupled stepwise in the presence of [*O*-(7-azabenzotriazol-1-yl)-1,1,3,3-tetramethyluronium hexafluorophosphate] (HATU) and DIPEA in DMF. At the end of peptide elongation, the alkene functions of the two allylglycines were cyclized via Ring Closing Metathesis (RCM), carried out with Hoveyda-Grubbs second generation catalyst in 1,2-dichloroethane under microwave irradiation.<sup>36-38</sup> This reaction, when used on solid phase, is associated with a pseudo-high dilution phenomena avoiding the undesirable formation of dimers.<sup>39</sup> To be noted, this step led to a mixture of unseparable (*E*) and (*Z*) isomers. Final resin cleavage with simultaneous side chain deprotection was performed with a mixture of trifluoroacetic acid (TFA)/H<sub>2</sub>O/triisopropylsilane (TIPS) (**Scheme 1**). The crude product, obtained after precipitation in *tert*-butyl methyl ether (TBME), was purified by reverse-phase chromatography, leading to the desired compounds with >95% purity, as determined by ultra-high performance liquid chromatography-mass spectrometry (UPLC-MS).

The design of the macrocyclic analogues of apelin-13 was based on the structure-activity relationship (SAR) described in the literature. The N-terminal residues Arg2-Pro3-Arg4-Leu5-Ser6 are important for binding to APJ.<sup>6,30</sup> Molecular modeling studies suggest that the Ser6 side chain would form a hydrogen bond with the Leu5 backbone carbonyl group thus stabilizing a  $\beta$ -turn, a conformation that favours interactions with the APJ receptor.<sup>27</sup> The C-terminal Phe13 residue of apelin-13 also plays a pivotal role, since it can modulate affinity for APJ, recruitment of  $\beta$ -arrestins, and is crucial for receptor internalization.<sup>6,28,30,31</sup> Therefore, apelin-13 possesses two distant pharmacophores that constitute the scaffold of this series of macrocycles. The alanine scan performed by Medhurst *et al.* showed that His7Ala and Met11Ala mutations in apelin-13 have no impact on binding and signalling.<sup>6</sup> With this in mind, we replaced these amino acids by allylglycine residues, pivotal for RCM, thereby positioning the macrocycle between the two important epitopes of apelin-13 as described in **Table 1**. Finally, Pro12 residue was initially removed and the N-terminal Pyr1 residue was deleted considering its lack of influence for APJ interaction.<sup>6</sup> Gratifyingly, compound **1** exhibited an affinity in the nM range with a 20-fold loss versus apelin-13 ( $K_i$  7.1 nM and 0.37 nM, respectively). This represents a good starting point, confirming that the macrocycle is well positioned and the global analogue conformation still fits into the binding pocket of APJ. The subsequent sections describe SAR investigation around this macrocyclic template.

### Modifications of the exocyclic C-terminal residue

We previously described that the C-terminal Phe13 residue of apelin-13 is a key modulator of binding affinity as well as cAMP and  $\beta$ -arrestin2 signalling.<sup>29-31</sup> To better understand

the role of this residue, we synthesized analogues where the C-terminus Phe was replaced by O-benzyl-Tyrosine (Tyr(OBn)), Ala or deleted, respectively compounds **2-4** (**Table 1**). Interestingly, the absence of aromatic side chain does not impact affinity for APJ (**3**,  $K_i$  9.6 nM vs **1**,  $K_i$  7.1 nM), which contrasts with the Phe13Ala substitution in linear apelin-13 that led to a >10-fold loss in binding.<sup>6</sup> Likewise, the lack of the C-terminal residue only slightly decreased affinity (**4**,  $K_i$  16 nM) suggesting that this series of macrocycles possibly interacts with the C-terminal pocket of APJ in slightly different ways compared to the apelin-13 native peptide. The Tyr(OBn) residue was then selected to replace the Phe amino acid. Indeed, in apelin-13, this modification led to an analogue with an affinity in the pM range (20 pM), a 60-fold improvement versus the native peptide.<sup>30</sup> The higher volume and  $\pi$ -stacking abilities of Tyr(OBn) seem to fit well in the C-terminal pocket of APJ, which has been suggested to be wide and rich in aromatic residues.<sup>28,40</sup> This observation remained true in this study since compound **2** exhibits a 4-fold increase in binding affinity compared to compound **1** (**2**,  $K_i$  1.7 nM) (**Table 1**). The Tyr(OBn) was therefore used as the C-terminal residue in the following series of analogues studied in this work.

### **Influence of the Tyr(OBn) position within the macrocycle and introduction of linkers**

We next examined whether the exocyclic position of the Tyr(OBn) residue in the macrocycle is optimal for APJ interaction. Thus, compounds **5** and **6** were synthesized, in which the Tyr(OBn) was endocyclic and introduced respectively between the Gly and Pro residues or between the Lys and Gly residues, thus increasing the size of the ring from 17- to 20-membered. As shown in **Table 2**, the pharmacodynamic consequences were substantial, and translated into a considerable drop in binding affinity close to a 20-fold



and a 400-fold loss compared to that of **2** (**5**,  $K_i$  29 nM; **6**,  $K_i$  662 nM vs **2**,  $K_i$  1.7 nM). The distance between the two epitopes and the ring conformational rearrangements induced by the Lys-Gly-Pro moiety seem to be better tolerated by the orthosteric site of APJ receptor. Overall, in this series, keeping the Tyr(OBn) residue in exocyclic position appeared to be the most promising option for further SAR analysis. Although several studies strongly suggested that Arg2-Pro3-Arg4-Leu5-Ser6 residues of apelin-13 are crucial for APJ interaction,<sup>26,27</sup> we found here that this N-terminal portion is not sufficient to account for peptide binding.

To further probe the C-terminal end of these new macrocyclic analogues of apelin-13, different amino acids inducing variable conformations and having different size were introduced as linkers between the ring and the Tyr(OBn) residue (**Table 3**). Compounds **7** and **10** displayed Pro or Ala residue as spacer, presumably imposing different backbone conformations in the macrocyclic peptides. Surprisingly, affinity for APJ was barely influenced by these modifications compared to the parent macrocycle **2** (**7**,  $K_i$  3.4 nM; **10**,  $K_i$  1.7 nM versus **2**,  $K_i$  1.7 nM). Likewise, compounds **8** and **9**, bearing respectively the more flexible  $\beta$ Ala and  $\gamma$ Abu spacers, exhibited binding affinity profiles for the APJ receptor in the same range as compound **2** or apelin-13 (**8**,  $K_i$  0.49 nM; **9**,  $K_i$  7.1 nM). Altogether, these results suggest that several solutions can be considered for positioning the critical C-terminal aromatic amino acid in the binding pocket of the APJ receptor.<sup>29,30,41</sup>

### Modifications of endocyclic positions

The size, rigidity and nature of endocyclic amino acids are crucial determinants for the interaction with APJ for this series. We modified the cycle as described in **Table 4**. We

synthesized analogues where the endocyclic Lys-Gly-Pro moiety was replaced by 8-aminocaprylic acid and  $\beta$ Ala- $\beta$ Ala residues with Tyr(OBn) and Pro-Tyr(OBn) amino acids at the C-terminal end (compounds **11-13**). These chemical modifications provoked an important perturbation in the nature of the ring, making it more flexible and lipophilic. Compound **11** exhibited a slightly decreased affinity compared to **2** (**11**,  $K_i$  11 nM vs **2**,  $K_i$  1.7 nM) which is surprising considering the important conformational changes induced by the 8-aminocaprylic acid residue. However, compounds **12** and **13** led to a substantial drop in binding affinity (**12**,  $K_i$  790 nM, **13**,  $K_i$  >10000 nM) compared to that of **2** and **11**. The presence of a peptide bond within the  $\beta$ Ala- $\beta$ Ala fragment is expected to introduce a local geometrical constraint compared to the 8-aminocaprylic acid, which appears to be deleterious for interactions with APJ. Additionally, the C-terminal Pro-Tyr(OBn) residue also seems to negatively impact the affinity compared to a unique Tyr(OBn) amino acid. To assess whether the cationic side chain of the endocyclic Lysine is important for APJ receptor binding, this residue was replaced by a norleucine (Nle, compound **14**, **Table 4**). Compared to **2**, **14** elicited a 30-fold loss of binding affinity (**14**,  $K_i$  53 nM), suggesting that the Lys residue is critical for receptor binding. One can hypothesize that the amine function is engaged in a polar interaction with APJ. Overall, these results demonstrated that the macrocycle is of primary importance for receptor interaction in this template, and plays a pivotal role for positioning the C-terminal residue in the binding pocket of APJ, a key pharmacophore to trigger signalling pathways. Nevertheless, the way the macrocycle docks into the receptor remains to be determined.

### N-terminal SAR study

The SAR study was completed by targeting the N-terminal peptidic moiety, Arg-Pro-Arg-Leu-Ser. Nuclear magnetic resonance (NMR) and circular dichroism (CD) studies suggested that the two Arg side chains of apelin-13 could be implicated in electrostatic interactions with Asp20 and Glu23 residues of APJ. Furthermore, this group speculated that the guanidine functions would be separated from each other by approximately 9 Å.<sup>42</sup> We were thus interested to determine if the guanidines of the two Arg residues are essential to maintain a good affinity for APJ. Starting from reference compound **2**, arginines were replaced by two Lys or Orn residues (**15** and **16**, **Table 5**). These modifications led to a slight decrease on receptor binding compared to **2** (**15**,  $K_i$  6.9 nM, **16**,  $K_i$  7.3 nM *versus* **2**,  $K_i$  1.7 nM). The difference of side chains length between Orn and Lys seems to have a neutral effect on interactions with APJ. However, considering that H-bond abilities of amines are lower than that of guanidines, these results suggest that interactions of Arg residues would be more electrostatic, thus enhancing the hypothesis of Langelann *et al.*<sup>42</sup> Furthermore, N-terminal truncation of **2**, leading to analogues **17** (deletion of N-terminal Arg-Pro residues) and **18** (deletion of N-terminal Arg-Pro-Arg-Leu-Ser residues), induced a marked reduction in receptor binding, showing respectively 150-fold and close to 1000-fold lower affinities compared to **2** (**17**,  $K_i$  258 nM, **18**,  $K_i$  1642 nM). Despite their lower affinity for APJ, these results open promising avenues for this macrocyclic template since similar linear peptidic analogues were reported to possess much lower affinities.<sup>30</sup> Indeed, compound **17** with only one Arg residue maintains a submicromolar affinity. Surprisingly, the macrocyclic moiety with the C-terminal Tyr(OBn) residue, analogue **18**, was still able to bind to APJ, in sharp contrast with previously described N-terminal truncated analogues of apelin-13 in which the deletion of Pyr1-Arg2-Pro3-Arg4-Leu5 completely abrogated the

binding for APJ.<sup>30</sup> These results further reinforce our hypothesis that this macrocyclic series of analogues interacts with the orthosteric pocket of the APJ receptor *via* binding sites topologically distinct from the endogenous ligand. Finally, to probe the importance of the N-terminal amine function, compounds **19-21** were synthesized (**Table 5**). The addition of a pyroglutamic acid (Pyr) residue or the acetylation of the primary amine elicited a minor drop in binding affinity compared to **2** (**19**,  $K_i$  6.2 nM, **20**,  $K_i$  3.4 nM). However, the desamino-Arg analogue **21** exhibited a drastic 65-fold decrease on receptor binding (**21**,  $K_i$  113 nM). Altogether, these results suggest that the N-terminal amine can be modified, however it retains some level of interaction with APJ.

#### Assessment of APJ receptor-mediated G-protein activation and $\beta$ -arrestin recruitment

The signalling profile of this novel series of macrocyclic analogues of apelin-13 was assessed, with an emphasis on  $G\alpha_{i1}$  and  $G\alpha_{oA}$  dissociation and recruitment of  $\beta$ -arrestins 1 and 2 in HEK293 cells stably expressing the human APJ receptor using Bioluminescence Resonance Energy Transfer (BRET)-based biosensors.<sup>43,44</sup> Following apelin-13 stimulation, dose-response curves for  $G\alpha_{i1}$ ,  $G\alpha_{oA}$ ,  $\beta$ -arrestin1 and  $\beta$ -arrestin2 exhibited half-maximal responses ( $EC_{50}$ ) respectively of 1.0, 2.3, 73 and 69 nM, as represented in **Figure 2**. Despite a binding affinity close to that of apelin-13, reference compound **2** was associated with a substantial loss in second messenger signalling compared to apelin-13 ( $G\alpha_{i1}$  35 nM;  $G\alpha_{oA}$  27 nM;  $\beta$ -arr1 553 nM;  $\beta$ -arr2 893 nM) (**Table 6**). The endocyclic position of the Tyr(OBn) residue, analogue **5**, induced an important loss in  $\beta$ -arrestin recruitment (**5**,  $EC_{50}$  >10000 nM). Similarly to binding studies, in this series of

macrocycles, the exocyclic configuration of the aromatic C-terminal amino acid seems to be optimal to maintain the pharmacodynamic profile. Introduction of linkers between the ring and the C-terminal residue also modulated the activation of the signalling pathways. Indeed, a slight improvement in potency was observed for **8** (linker:  $\beta$ Ala) versus **2**. On the other hand, we observed almost a 10-fold drop in signalling for analogue **9** (linker:  $\gamma$ Abu) compared to **8** ( $G\alpha_{i1}$  130 nM;  $G\alpha_{oA}$  103 nM;  $\beta$ -arr1 5602 nM;  $\beta$ -arr2 4656 nM). This linker impaired both binding and signalling, suggesting that the distance from the ring and orientation of the C-terminal residue are critical for both G-protein-dependent and -independent pathways. Modifications of the ring, the C- and N-terminal moiety led to the discovery of analogues **4**, **11**, and **15** which trigger  $G\alpha_{i1}$  and  $G\alpha_{oA}$  subunits (**4**,  $G\alpha_{i1}$  62 nM;  $G\alpha_{oA}$  64 nM, **11**,  $G\alpha_{i1}$  190 nM;  $G\alpha_{oA}$  174 nM and **15**,  $G\alpha_{i1}$  56 nM;  $G\alpha_{oA}$  50 nM), with no recruitment of  $\beta$ -arrestins (**4**, **11**, and **15**,  $\beta$ -arr 1 & 2 >10000 nM) (**Figure 2**, **Table 6**). Furthermore, compounds **4**, **11**, and **15** were able to bind to APJ in the nM range (**Table 4** and **5**). Therefore, these macrocyclic analogues exhibit a functional selectivity toward G-protein activation over  $\beta$ -arrestin signalling.<sup>45</sup> Compounds **4**, **11**, and **15** are the first reported apelin analogues that possess such a strong bias toward G-protein activation while maintaining an affinity close to that of apelin-13. These molecules thus represent powerful pharmacological tools to better understand the link between signalling pathways and physiological effects, which will be reported in due course.

### Effects on blood pressure following bolus administration

Previous studies demonstrated that apelin-13 can lower mean arterial blood pressure (MAP) in normal and spontaneously hypertensive rats when administered in bolus,<sup>25,30,46</sup>

although this was not the case with continuous infusion.<sup>47</sup> Additionally, the C-terminal amino acid of apelin has been shown to play a pivotal role in lowering the mean arterial pressure (MAP).<sup>30,31,46</sup> We thus investigated the effects of this series of macrocycles on the modulation of blood pressure, by focusing on compounds exhibiting the most interesting binding affinity profiles. Those selected derivatives are represented in bold in **Table 6** and their dose-response curves for each signalling pathway depicted in **Figure 2**. Analogues **2**, **7**, **8**, **15**, **19**, **20** and apelin-13 were administered intravenously at a dose of 19.6 nmol/kg to male Sprague-Dawley rats, and their arterial blood pressure monitored via direct continuous intra-carotid measurements. For each compound, the max  $\Delta$ MAP corresponding to the maximal drop in MAP was compared to rats treated with saline (**Figure 3**). Apelin-13 exerted a maximal hypotensive effect reaching -35 mmHg and analogue **8** induced a similar max  $\Delta$ MAP at the equimolar dose of 19.6 nmol/kg. Compounds **2** and **19** tended to induce a less intense max  $\Delta$ MAP compared to apelin-13 yet statistically significant *versus* rats receiving saline. Interestingly, analogues **15** and **20** provoked no hypotensive effect at all following i.v. administration. The rational between signalling and *in vivo* vascular effects for the apelinergic system are not completely understood. Indeed, previous studies suggested that the drop in MAP elicited by apelin analogues depends on the ability of those ligands to induce APJ internalization and consequently to recruit  $\beta$ -arrestins.<sup>15,31,46</sup> Analogues **15** and **20**, exhibiting  $EC_{50} > 5000$  nM to activate  $\beta$ -arrestins recruitment (**Table 6**) and inducing no statistically significant hypotensive effects are in phase with this hypothesis. However, further in-depth studies are required to fully understand this mechanism.

## Conclusion

In this study, we report the design and synthesis of a novel series of macrocyclic analogues of apelin-13. We conducted a SAR investigation of these molecules and evaluated their abilities to bind to APJ and activate the  $G\alpha_{i1}$  and  $G\alpha_{oA}$  subunits as well as to recruit  $\beta$ -arrestins1 and 2. Altogether, our results demonstrated that, in this macrocyclic template, the C-terminal residue is crucial in the modulation of binding and signalling, especially for  $\beta$ -arrestin recruitment. Indeed, the Tyr(OBn) amino acid, when replaced by a non-aromatic residue or when positioned within the ring, markedly influences the capacity of APJ to interact with  $\beta$ -arrestins. This observation is in agreement with current knowledge, as it was previously demonstrated for linear C-terminal modified apelin-13 derivatives that this residue already held such key role.<sup>30,31</sup> This study also led to the discovery of several new potent G protein-biased apelin receptor agonists, especially compounds **4**, **11**, and **15** which exhibit binding affinity profiles in the nanomolar range. Additionally, despite its modest affinity of 1642 nM, analogue **18** possesses a simplified chemical structure and represents a promising starting point for further studies in order to improve the biological properties of this set of macrocycles.

## Experimental

### Procedures for solid phase synthesis

#### Materials

Wang resin (4-benzyloxybenzyl alcohol resin) was purchased from ChemImpex International (USA). [O-(7-azabenzotriazol-1-yl)-1,1,3,3-tetramethyluronium hexafluorophosphate] (HATU) and Fmoc-protected (L)-amino acids were purchased from Matrix Innovation (Canada). Hoveyda-Grubbs catalyst 2nd generation was purchased from Sigma-Aldrich (Canada). All other reagents and solvents were purchased from Sigma-Aldrich (Canada), Fisher Scientific (USA) or ACP (Canada), and were of the highest commercially available purity. All reagents and starting materials were used as received. Peptide synthesis was performed in 12 mL polypropylene cartridge with 20  $\mu$ m PE frit from Applied Separations (USA).

#### Peptide synthesis

In a typical procedure, Wang resin (0.3 mmol/g, 0.3 g) was treated with triphenylphosphine (3 equiv), diisopropylazodicarboxylate (DIAD, 3 equiv) and Fmoc-protected amino acid (3 equiv) in tetrahydrofuran (THF, 5 mL). The mixture was shaken overnight on an orbital shaker at room temperature (RT), then the resin was sequentially washed for 3-min periods with DCM (2x 5 mL), 2-propanol (1x 5 mL), DCM (1x 5 mL), 2-propanol (1x 5 mL), DCM (2x 5 mL). A capping solution of DCM/Ac<sub>2</sub>O/DIPEA (20/5/1, 5 mL) was then added and the mixture shaken for 1 h at RT and washed with the above solvent sequence. After Fmoc



deprotection with 20% piperidine/DMF (*N,N*-dimethylformamide) (2x 10 min), the subsequent Fmoc-protected amino acid (5 equiv) was attached in the presence of HATU (5 equiv) and DIPEA (10 equiv) in DMF (5 mL). Coupling reaction proceeded for 30 min, unless the amino acid was being added to a Pro residue, in which case reaction lasted for 60 min. Piperidine (20% in DMF) was used to deprotect the Fmoc group at every step. The resin was washed after each coupling step and deprotection with the above sequence of solvents. At the end of the elongation, for the ring closing metathesis (RCM) reaction, the resin was transferred in a microwave reactor, dried under vacuum during 2 h, then flushed with Argon during 30 min. Hoveyda-Grubbs catalyst 2nd generation (0.2 equiv) was added, then the tube was flushed again with Argon during 15 min. Freshly distilled 1,2-dichloroethane (3 mL) was finally added, then the reaction was carried out in a microwave apparatus (Discover Activent 10/35mL from CEM, USA) during 1 h at 77°C. The resin was then sequentially washed with DCM (3x 5 mL), MeOH (3x 5 mL) then DCM (3x 5 mL). Final resin cleavage was performed using a mixture of TFA (trifluoroacetic acid)/H<sub>2</sub>O/TIPS (triisopropylsilane), 95/2.5/2.5, v/v (4 mL / 0.3 g of resin) for 4 h at RT. After filtration, the peptide was precipitated in *tert*-butyl methyl ether (TBME) at 0°C, the suspension was centrifuged, the supernatant removed and the crude product re-dissolved in aqueous AcOH 10%. Purification by reverse-phase HPLC yielded the desire products, isolated as white powders after lyophilization.

### **Peptide purification and characterization**

Crude peptides were purified by reverse-phase chromatography using a preparative HPLC from Waters (Autosampler 2707, Quaternary gradient module 2535, UV detector 2489,

fraction collector WFCIII) equipped with an ACE5 C<sub>18</sub> column (250 x 21.2 mm, 5 µm spherical particle size) and water + 0.1% TFA and acetonitrile as eluents. To determine purity, analytical UPLC chromatograms were recorded on a Waters Acquity H-Class equipped with an Acquity UPLC BEH C<sub>18</sub> column (1.7 µm particles size, 2.1 x 50 mm) using the following gradient: water + 0.1% TFA and acetonitrile (0→0.2 min: 5% acetonitrile; 0.2→1.5 min: 5%→95%; 1.5→1.8 min: 95%; 1.8 → 2.0 min: 95% → 5%; 2.0 → 2.5 min: 5%). All analogues possessed UV purity >95% and were characterized by mass spectrometry (Electrospray infusion ESI-Q-ToF from Maxis).

## **Binding affinity and signalling pathways**

### **Materials**

High glucose Dulbecco's Modified Eagle Medium (DMEM), G418 and penicillin/streptomycin were purchased from Invitrogen Life Technologies (Canada). Foetal bovine serum (FBS) was purchased from Wisent (Canada) and bovine serum albumin (BSA) from BioShop (Canada). White opaque 96-well half area plates were purchased from PerkinElmer (Canada). Polyethylenimine (branched PEI) was obtained from Polysciences (USA). Coelenterazine-400A (DeepBlueC) was purchased from Biosynth AG (Switzerland). BRET<sup>2</sup> measurements were performed on a GeniosPro plate reader from Tecan (Austria). Apelin-13[Glp<sup>65</sup>, Nle<sup>75</sup>, Tyr<sup>77</sup>][<sup>125</sup>I] (specific activity 820 Ci/mmol) was prepared using IODO-GEN (1,3,4,6-tetrachloro-3a, 6a-diphenyl-glycoluril; Thermo Scientific Pierce, Canada) as described by Fraker and Speck.<sup>48</sup> Briefly, 10 µL of a 1 mM peptide solution was incubated with 20 µg of IODO-GEN, 80 µL of 100 mM borate buffer

(pH 8.5), and 1 mCi of Na-<sup>125</sup>I for 30 min at RT, and was then purified by reversed-phase HPLC on a C<sub>18</sub> column. The specific radioactivity of the labeled peptide was determined by self-displacement and saturation-binding analysis.

### **Radioligand binding**

HEK293 cells expressing the YFP epitope-tagged human APJ were washed once with PBS and subjected to one freeze-thaw cycle. Broken cells were then gently scraped in resuspension buffer (1 mM EDTA and 10 mM Tris-HCl, pH 7.5), centrifuged at 3500 g for 15 min at 4°C and resuspended in binding buffer (50 mM Tris-HCl buffer, pH 7.5, containing 0.2% BSA). Competitive radioligand binding experiments were performed by incubating cell membranes (15 µg) with 0.2 nM Apelin-13[Glp<sup>65</sup>, Nle<sup>75</sup>, Tyr<sup>77</sup>][<sup>125</sup>I] (820 Ci/mmol) and increasing concentrations of various analogues (10<sup>-11</sup> to 10<sup>-5</sup> M) for 1 h at RT in a final volume of 200 µL. Bound radioactivity was separated from free ligand by filtration through GF/C glass fiber filter plates (Millipore, Billerica, MA) pre-soaked for 1 h in PEI 0.2% at 4°C and washed 3 times with 170 µL of ice-cold binding buffer. Receptor-bound radioactivity was counted in a γ-counter 1470 Wizard<sup>2</sup> form PerkinElmer (80% counting efficiency). Nonspecific binding was measured in the presence of 10<sup>-5</sup> M unlabeled apelin-13 and represented less than 5% of total binding. K<sub>i</sub> values were determined from dose-response curves as the unlabeled ligand concentration inhibiting 50% of [<sup>125</sup>I]-apelin-13 specific binding and using the Cheng-Prusoff equation.<sup>49</sup> All binding data were calculated and plotted using GraphPad Prism 6 (La Jolla, CA) and represent the mean ± SEM of three determinations.

## BRET experiments

HEK293 cells, seeded in T175 flasks, were allowed to grow in high glucose DMEM supplemented with 10% FBS, 100 U/mL penicillin/streptomycin, 2 mM glutamine, and 20 mM HEPES at 37°C in a humidified chamber at 5% CO<sub>2</sub>. All transfections were carried out with polyethylenimine.<sup>50</sup> After 24 h, cells were transfected with the plasmids coding for hAPJ, G $\alpha_{i1}$ -RlucII, GFP10-G $\gamma_1$ , G $\beta_1$  (from [www.cdna.org](http://www.cdna.org)) (for BRET based G $\alpha_{i1}$  activation assay) or hAPJ, G $\alpha_{oA}$ -RlucII, GFP10-G $\gamma_1$ , G $\beta_1$  (for BRET based G $\alpha_{oA}$  activation assay) or hAPJ-GFP10 and RlucII- $\beta$ arrestin1 or RlucII- $\beta$ arrestin2 (for BRET based  $\beta$ -arrestin recruitment) using polyethylenimine.<sup>30,43,44</sup> To perform the BRET assay, cells were transferred into white 96 well plates (BD Falcon) at a concentration of 50 000 cells/well 24 h after transfection and incubated at 37°C overnight. Cells were then washed with PBS and 90  $\mu$ L of HBSS was added in each well. Then, cells were stimulated with analogues at concentrations ranging from 10<sup>-5</sup> M to 10<sup>-11</sup> M for 5 min at 37°C (G $\alpha_{i1}$  and G $\alpha_{oA}$ ) or for 30 min at RT ( $\beta$ -arrestin1 and 2). After stimulation, 5  $\mu$ M of coelenterazine 400A was added to each well and the plate was read using the BRET<sup>2</sup> filter set of a GeniosPro plate reader (Tecan, Austria). The BRET<sup>2</sup> ratio was determined as GFP10<sub>em</sub>/RlucII<sub>em</sub>. Data were plotted and EC<sub>50</sub> values were determined using GraphPad Prism 6. Each data point represents the mean  $\pm$  SEM of at least three different experiments each done in triplicate.

## Animals

Adult male Sprague Dawley rats (Charles River Laboratories, St-Constant, Quebec, Canada) were maintained on a 12 h light/12 h dark cycle with access to food and water *ad libitum*. The animal experimental procedures in this study were approved by the Animal

Care Committee of Université de Sherbrooke and were in accordance with policies and directives of the Canadian Council on Animal Care.

### **Hypotensive effects**

Rats were anaesthetized with a mixture of ketamine/xylazine (87 mg/kg : 13 mg/kg, i.m.) and placed in supine position on a heating pad. Mean, systolic, and diastolic arterial blood pressure, as well as heart rate, were measured through a catheter (PE 50 filled with heparinized saline) inserted in the right carotid artery and connected to a Micro-Med transducer (model TDX-300, USA) linked to a blood pressure Micro-Med analyzer (model BPA-100c). Another catheter was inserted into the left jugular vein for bolus injections (1 mL/kg, 5-10 s) of vehicle (isotonic saline), or analogues at dose of 19.6 nmol/kg. Rats were given vehicle first, then only one dose of a single analogue prior to euthanasia. For relative potency evaluation, changes in blood pressure from baseline to maximal effect post-injection in individual animals were determined. Data represents mean  $\pm$  SEM of at least six different experiments.

## Acknowledgements

Financial support from Université de Sherbrooke, the Natural Sciences and Engineering Research Council of Canada, the Canada Foundation for Innovation, Merck Sharpe & Dohme (donation to the Faculty of Medicine and Health Sciences of Université de Sherbrooke) and the FRQS-funded Réseau Québécois de Recherche sur le Médicament (RQRM) is acknowledged. The Institut de Pharmacologie de Sherbrooke (IPS) and MITACS are also acknowledged for scholarship grants to A.M and X.S. M.A.-M. is the recipient of a Heart and Stroke Foundation of Canada (HSFC) New Investigator award. P.S. is the recipient of the Canada Research Chair in Neurophysiopharmacology of Chronic Pain. E.M. is a member of the FRQNT-funded Proteo Network. The authors would also like to thank Prof. Michel Bouvier (Institut de Recherche en Immunologie et Cancer, Montréal, Québec, Canada) for the use of human  $G\alpha_{i1}$ ,  $G\alpha_{oA}$ , and  $\beta$ -arrestin biosensors.

## Bibliographic references & notes

- 1 B. F. O'Dowd, M. Heiber, A. Chan, H. H. Heng, L. C. Tsui, J. L. Kennedy, X. Shi, A. Petronis, S. R. George and T. Nguyen, *Gene*, 1993, **136**, 355–60.
- 2 K. Tatemoto, M. Hosoya, Y. Habata, R. Fujii, T. Kakegawa, M. X. Zou, Y. Kawamata, S. Fukusumi, S. Hinuma, C. Kitada, T. Kurokawa, H. Onda and M. Fujino, *Biochem. Biophys. Res. Commun.*, 1998, **251**, 471–6.
- 3 D. L. Lee, R. Cheng, T. Nguyen, T. Fan, A. P. Kariyawasam, Y. Liu, D. H. Osmond, S. R. George and B. F. O'Dowd, *J. Neurochem.*, 2000, **74**, 34–41.
- 4 Y. Habata, R. Fujii, M. Hosoya, S. Fukusumi, Y. Kawamata, S. Hinuma, C. Kitada, N. Nishizawa, S. Murosaki, T. Kurokawa, H. Onda, K. Tatemoto and M. Fujino, *Biochim. Biophys. Acta*, 1999, **1452**, 25–35.
- 5 E. Y. Zhen, R. E. Higgs and J. a Gutierrez, *Anal. Biochem.*, 2013, **442**, 1–9.
- 6 A. D. Medhurst, C. a Jennings, M. J. Robbins, R. P. Davis, C. Ellis, K. Y. Winborn, K. W. M. Lawrie, G. Hervieu, G. Riley, J. E. Bolaky, N. C. Herrity, P. Murdock and J. G. Darker, *J. Neurochem.*, 2003, **84**, 1162–1172.
- 7 M. Hosoya, Y. Kawamata, S. Fukusumi, R. Fujii, Y. Habata, S. Hinumat, C. Kitada, S. Honda, T. Kurokawa, H. Onda, O. Nishimura and M. Fujino, *J. Biol. Chem.*, 2000, **275**, 21061–21067.
- 8 A. M. O'Carroll, T. L. Selby, M. Palkovits and S. J. Lolait, *Biochim. Biophys. Acta - Gene Struct. Expr.*, 2000, **1492**, 72–80.
- 9 I. Falcão-Pires, R. Ladeiras-Lopes and A. F. Leite-Moreira, *Expert Opin. Ther.*

- Targets*, 2010, **14**, 633–45.
- 10 A.-M. O’Carroll, S. J. Lolait, L. E. Harris and G. R. Pope, *J. Endocrinol.*, 2013, **219**, R13-35.
- 11 M. C. Scimia, C. Hurtado, S. Ray, S. Metzler, K. Wei, J. Wang, C. E. Woods, N. H. Purcell, D. Catalucci, T. Akasaka, O. F. Bueno, G. P. Vlasuk, P. Kaliman, R. Bodmer, L. H. Smith, E. Ashley, M. Mercola, J. H. Brown and P. Ruiz-Lozano, *Nature*, 2012, **488**, 394–8.
- 12 C. Chamberland, H. Barajas-Martinez, V. Haufe, M.-H. Fecteau, J.-F. Delabre, A. Burashnikov, C. Antzelevitch, O. Lesur, A. Chraibi, P. Sarret and R. Dumaine, *J. Mol. Cell. Cardiol.*, 2010, **48**, 694–701.
- 13 M. F. Berry, T. J. Pirolli, V. Jayasankar, J. Burdick, K. J. Morine, T. J. Gardner and Y. J. Woo, *Circulation*, 2004, **110**, II187-93.
- 14 I. Szokodi, P. Tavi, G. Földes, S. Voutilainen-Myllylä, M. Ilves, H. Tokola, S. Pikkarainen, J. Piuhola, J. Rysä, M. Tóth and H. Ruskoaho, *Circ. Res.*, 2002, **91**, 434–440.
- 15 S. El Messari, X. Iturrioz, C. Fassot, N. De Mota, D. Roesch and C. Llorens-Cortes, *J. Neurochem.*, 2004, **90**, 1290–301.
- 16 A. G. Japp, N. L. Cruden, D. a B. Amer, V. K. Y. Li, E. B. Goudie, N. R. Johnston, S. Sharma, I. Neilson, D. J. Webb, I. L. Megson, A. D. Flapan and D. E. Newby, *J. Am. Coll. Cardiol.*, 2008, **52**, 908–13.
- 17 a G. Japp, N. L. Cruden, G. Barnes, N. van Gemeren, J. Mathews, J. Adamson, N. R. Johnston, M. a Denvir, I. L. Megson, a D. Flapan and D. E. Newby, *Circulation*, 2010, **121**, 1818–27.



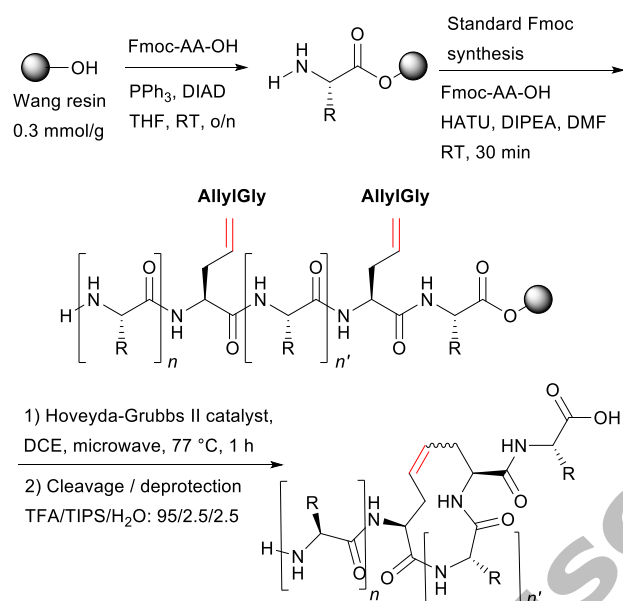
- 18 J. Hamada, J. Kimura, J. Ishida, T. Kohda, S. Morishita, S. Ichihara and A. Fukamizu, *Int. J. Mol. Med.*, 2008, **22**, 547–52.
- 19 C. D’Aniello, E. Lonardo, S. Iaconis, O. Guardiola, A. M. Liguoro, G. L. Liguori, M. Autiero, P. Carmeliet and G. Minchiotti, *Circ. Res.*, 2009, **105**, 231–8.
- 20 P. Yue, H. Jin, S. Xu, M. Aillaud, A. C. Deng, J. Azuma, R. K. Kundu, G. M. Reaven, T. Quertermous and P. S. Tsao, *Endocrinology*, 2011, **152**, 59–68.
- 21 D. K. Lee, S. S. G. Ferguson, S. R. George and B. F. O’Dowd, *Biochem. Biophys. Res. Commun.*, 2010, **395**, 185–9.
- 22 S. C. Chng, L. Ho, J. Tian and B. Reversade, *Dev. Cell*, 2013, **27**, 672–80.
- 23 A. Pauli, M. L. Norris, E. Valen, G.-L. Chew, J. a Gagnon, S. Zimmerman, A. Mitchell, J. Ma, J. Dubrulle, D. Reyon, S. Q. Tsai, J. K. Joung, A. Saghatelian and A. F. Schier, *Science*, 2014, 1–13.
- 24 Z. Wang, D. Yu, M. Wang, Q. Wang, J. Kouznetsova, R. Yang, K. Qian, W. Wu, A. Shuldiner, C. Sztalryd, M. Zou, W. Zheng and D.-W. Gong, *Sci. Rep.*, 2015, **5**, 8170.
- 25 A. Murza, X. Sainsily, D. Coquerel, J. Côté, P. Marx, É. Besserer-Offroy, J.-M. Longpré, J. Lainé, B. Reversade, D. Salvail, R. Leduc, R. Dumaine, O. Lesur, M. Auger-Messier, P. Sarret and É. Marsault, *J. Med. Chem.*, 2016, **59**, 2962–2972.
- 26 D. N. Langelaan, E. M. Bebbington, T. Reddy and J. K. Rainey, *Biochemistry*, 2009, **48**, 537–548.
- 27 N. J. M. Macaluso and R. C. Glen, *ChemMedChem*, 2010, **5**, 1247–53.
- 28 X. Iturrioz, R. Gerbier, V. Leroux, R. Alvear-Perez, B. Maigret and C. Llorens-Cortes, *J. Biol. Chem.*, 2010, **285**, 32627–37.

- 29 A. Murza, A. Parent, E. Besserer-Offroy, H. Tremblay, F. Karadereye, N. Beaudet, R. Leduc, P. Sarret and É. Marsault, *ChemMedChem*, 2012, **7**, 318–325.
- 30 A. Murza, É. Besserer-Offroy, J. Côté, P. Bérubé, J.-M. Longpré, R. Dumaine, O. Lesur, M. Auger-Messier, R. Leduc, P. Sarret and É. Marsault, *J. Med. Chem.*, 2015, **58**, 2431–40.
- 31 E. Ceraudo, C. Galanth, E. Carpentier, I. Banegas-Font, A.-M. Schonegge, R. Alvear-Perez, X. Iturrioz, M. Bouvier and C. Llorens-Cortes, *J. Biol. Chem.*, 2014, **289**, 24599–610.
- 32 S. Narayanan, D. L. Harris, R. Maitra and S. P. Runyon, *J. Med. Chem.*, 2015, **58**, 7913–7927.
- 33 C.G. Wermuth, *The Practice of Medicinal Chemistry*, Elsevier/Academic Press, London, 2008.
- 34 N. J. M. Macaluso, S. L. Pitkin, J. J. Maguire, A. P. Davenport and R. C. Glen, *ChemMedChem*, 2011, **6**, 1017–23.
- 35 A. L. Brame, J. J. Maguire, P. Yang, A. Dyson, R. Torella, J. Cheriyan, M. Singer, R. C. Glen, I. B. Wilkinson and A. P. Davenport, *Hypertension*, 2015, **65**, 834–40.
- 36 S. J. Miller, H. E. Blackwell and R. H. Grubbs, *J. Am. Chem. Soc.*, 1996, **118**, 9606–9614.
- 37 S. B. Garber, J. S. Kingsbury, B. L. Gray and A. H. Hoveyda, *J. Am. Chem. Soc.*, 2000, **122**, 8168–8179.
- 38 A. Patgiri, M. Z. Menzenski, A. B. Mahon and P. S. Arora, *Nat. Protoc.*, 2010, **5**, 1857–65.
- 39 M. J. Pérez de Vega, M. I. García-Aranda and R. González-Muñiz, *Med. Res. Rev.*,

- 2011, **31**, 677–715.
- 40 R. Gerbier, V. Leroux, P. Couvineau, R. Alvear-Perez, B. Maigret, C. Llorens-Cortes and X. Iturrioz, *FASEB J.*, 2015, **29**, 314–22.
- 41 J.-F. Margathe, X. Iturrioz, R. Alvear-Perez, C. Marsol, S. Riché, H. Chabane, N. Tounsi, M. Kuhry, D. Heissler, M. Hibert, C. Llorens-Cortes and D. Bonnet, *J. Med. Chem.*, 2014, **57**, 2908–19.
- 42 D. N. Langelan, T. Reddy, A. W. Banks, G. Dellaire, D. J. Dupré and J. K. Rainey, *Biochim. Biophys. Acta*, 2013, **1828**, 1471–83.
- 43 B. Zimmerman, A. Beautrait, B. Aguila, R. Charles, E. Escher, A. Claing, M. Bouvier and S. A. Laporte, *Sci. Signal.*, 2012, **5**, ra33.
- 44 C. Galés, J. J. J. Van Durm, S. Schaak, S. Pontier, Y. Percherancier, M. Audet, H. Paris and M. Bouvier, *Nat. Struct. Mol. Biol.*, 2006, **13**, 778–86.
- 45 D. H. Rominger, C. L. Cowan, W. Gowen-MacDonald and J. D. Violin, *Curr. Opin. Pharmacol.*, 2014, **16C**, 108–115.
- 46 D. K. Lee, V. R. Saldivia, T. Nguyen, R. Cheng, S. R. George and B. F. O’Dowd, *Endocrinology*, 2005, **146**, 231–6.
- 47 F. Chagnon, D. Coquerel, D. Salvail, E. Marsault, R. Dumaine, M. Auger-Messier, P. Sarret and O. Lesur, *Crit. Care Med.*, 2016, 1.
- 48 P. J. Fraker and J. C. Speck, *Biochem. Biophys. Res. Commun.*, 1978, **80**, 849–857.
- 49 Y. Cheng and W. H. Prusoff, *Biochem. Pharmacol.*, 1973, **22**, 3099–108.
- 50 C. Ehrhardt, M. Schmolke, A. Matzke, A. Knoblauch, C. Will, V. Wixler and S. Ludwig, *Signal Transduct.*, 2006, **6**, 179–184.

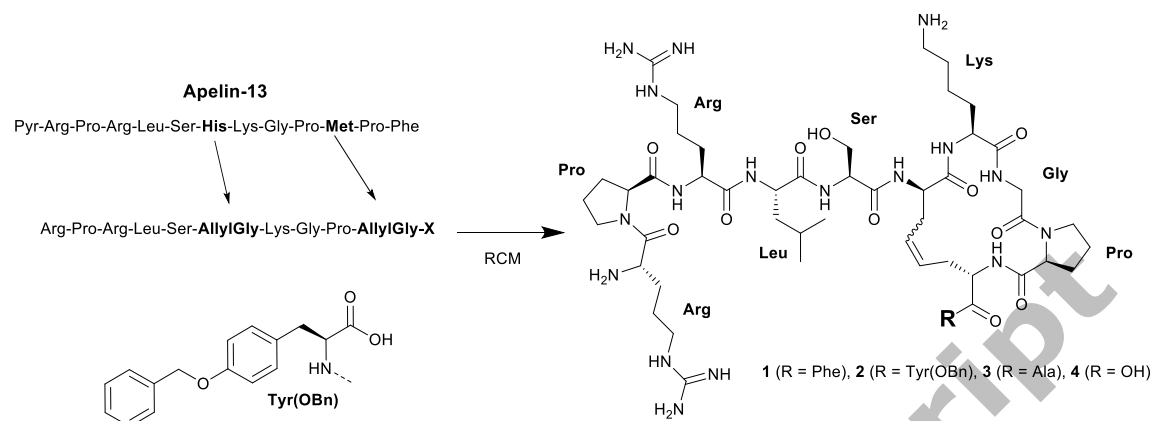
**This is the accepted (postprint) version of the following article:** Murza A, *et al.* (2017). *Org Biomol Chem.* doi: 10.1039/c6ob02247b, **which has been accepted and published in its final form at** <http://pubs.rsc.org/en/Content/ArticleLanding/2017/OB/C6OB02247B>

Accepted Manuscript



**Scheme 1.** Synthesis of macrocyclic analogues of apelin-13

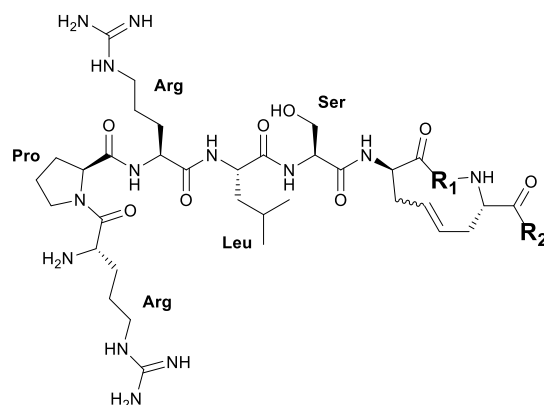
**Table 1.** Modifications of the C-terminal exocyclic residue



Compounds	R	Cycle size	Binding $K_i$ (nM) <sup>a</sup>
Apelin-13			$0.37 \pm 0.04$
1	Phe	17	$7.1 \pm 1.8$
2	Tyr(OBn)	17	$1.7 \pm 0.25$
3	Ala	17	$9.6 \pm 1.1$
4	-OH	17	$16 \pm 3.1$

<sup>a</sup> Binding constants ( $K_i$ ) calculated from measured radioligand binding  $IC_{50}$  values using the Cheng-Prusoff equation, values represent the mean  $\pm$  SEM of three determinations.

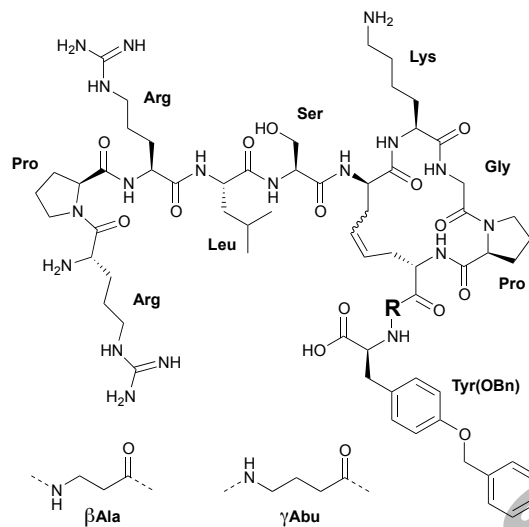
**Table 2.** Influence of the Tyr(OBn) position within the cycle



Compounds	R <sub>1</sub>	R <sub>2</sub>	Cycle size	Binding $K_i$ (nM) <sup>a</sup>
Apelin-13	--			0.37 ± 0.04
<b>2</b>	Lys-Gly-Pro	<b>Tyr(OBn)</b>	17	1.7 ± 0.25
<b>5</b>	Lys-Gly- <b>Tyr(OBn)</b> -Pro	-OH	20	29 ± 2.5
<b>6</b>	Lys- <b>Tyr(OBn)</b> -Gly-Pro	-OH	20	662 ± 128

<sup>a</sup> Binding constants ( $K_i$ ) calculated from measured radioligand binding  $IC_{50}$  values using the Cheng-Prusoff equation, values represent the mean ± SEM of three determinations.

**Table 3.** Introduction of linkers between the cycle and Tyr(OBn)

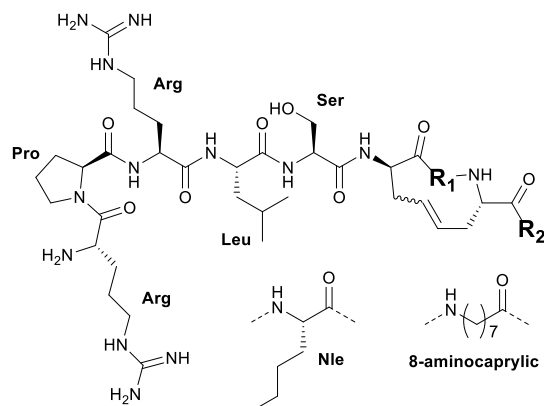


Compounds	R	Cycle size	Binding $K_i$ (nM) <sup>a</sup>
Apelin-13	–	–	$0.37 \pm 0.04$
<b>2</b>	--	17	$1.7 \pm 0.25$
<b>7</b>	Pro	17	$3.4 \pm 0.68$
<b>8</b>	$\beta$ Ala	17	$0.49 \pm 0.12$
<b>9</b>	$\gamma$ Abu	17	$7.1 \pm 1.5$
<b>10</b>	Ala	17	$3.3 \pm 1.6$

<sup>a</sup> Binding constants ( $K_i$ ) calculated from measured radioligand binding  $IC_{50}$  values using the Cheng-Prusoff equation, values represent the mean  $\pm$  SEM of three determinations.



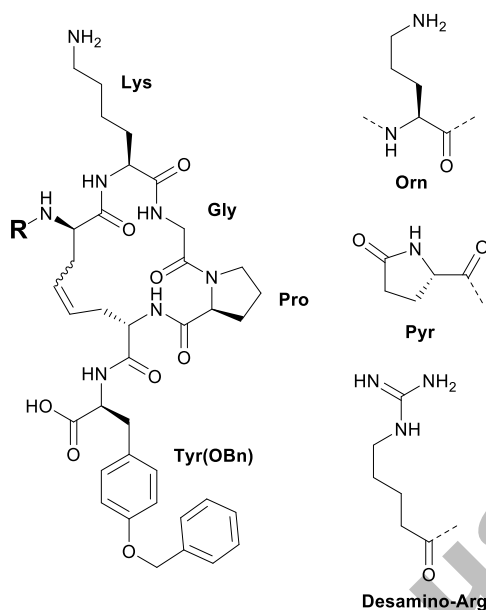
**Table 4.** Modifications of endocyclic positions



Compounds	R <sub>1</sub>	R <sub>2</sub>	Cycle size	Binding $K_i$ (nM) <sup>a</sup>
Apelin-13	--	--		0.37 ± 0.04
<b>2</b>	Lys-Gly-Pro	Tyr(OBn)	17	1.7 ± 0.25
<b>11</b>	8-aminocaprylic	Pro-Tyr(OBn)	17	11 ± 3.4
<b>12</b>	βAla-βAla	Tyr(OBn)	16	790 ± 107
<b>13</b>	βAla-βAla	Pro-Tyr(OBn)	16	>10000
<b>14</b>	Nle-Gly-Pro	Tyr(OBn)	17	53 ± 8.1

<sup>a</sup> Binding constants ( $K_i$ ) calculated from measured radioligand binding  $IC_{50}$  values using the Cheng-Prusoff equation, values represent the mean ± SEM of three determinations.

**Table 5.** N-terminal SAR



Compounds	R	Cycle size	Binding $K_i$ (nM) <sup>a</sup>
Apelin-13	--		0.37 ± 0.04
<b>2</b>	Arg-Pro-Arg-Leu-Ser	17	1.7 ± 0.25
<b>15</b>	Lys-Pro-Lys-Leu-Ser	17	6.9 ± 0.77
<b>16</b>	Orn-Pro-Orn-Leu-Ser	17	7.3 ± 3.1
<b>17</b>	Arg-Leu-Ser	17	258 ± 47
<b>18</b>	-H	17	1642 ± 797
<b>19</b>	Pyr-Arg-Pro-Arg-Leu-Ser	17	6.2 ± 1.3
<b>20</b>	Ac-Arg-Pro-Arg-Leu-Ser	17	3.4 ± 1.1
<b>21</b>	Desamino-Arg-Pro-Arg-Leu-Ser	17	113 ± 28

<sup>a</sup> Binding constants ( $K_i$ ) calculated from measured radioligand binding  $IC_{50}$  values using the Cheng-Prusoff equation, values represent the mean ± SEM of three determinations.

**Table 6.** Effect of macrocycles on  $G\alpha_{i1}$  and  $G\alpha_{oA}$  activation as well as  $\beta$ -arrestin1 and 2 recruitment

	$G\alpha_{i1}$	$G\alpha_{oA}$	$\beta$ -arrestin1	$\beta$ -arrestin2
	$EC_{50}$ (nM) <sup>a</sup>			
Apelin-13	1,0 ± 0,2	2,3 ± 0,2	73 ± 4,8	69 ± 12
1	59 ± 14	189 ± 63	>10000	>10000
<b>2</b>	<b>35 ± 11</b>	<b>27 ± 32</b>	<b>553 ± 27</b>	<b>893 ± 262</b>
3	7,5 ± 3,2	22 ± 11	622 ± 30	657 ± 198
4	62 ± 18	64 ± 2,2	>10000	>10000
5	82 ± 12	156 ± 23	>10000	>10000
6	-	-	-	-
7	<b>22 ± 7,4</b>	<b>30 ± 8</b>	<b>836 ± 132</b>	<b>854 ± 193</b>
<b>8</b>	<b>24 ± 8,5</b>	<b>21 ± 7,1</b>	<b>457 ± 17</b>	<b>524 ± 126</b>
9	130 ± 45	146 ± 76	5602 ± 863	4656 ± 706
10	62 ± 16	95 ± 23	1399 ± 413	2279 ± 606
11	190 ± 38	174 ± 47	>10000	>10000
12	-	-	-	-
13	> 10000	> 10000	>10000	>10000
14	87 ± 25	110 ± 22	2512 ± 781	2646 ± 334
<b>15</b>	<b>56 ± 8,8</b>	<b>50 ± 12</b>	<b>&gt;10000</b>	<b>&gt;10000</b>
16	234 ± 38	332 ± 83	>10000	>10000
17	-	-	-	-
18	-	-	-	-
<b>19</b>	<b>33 ± 6,0</b>	<b>35 ± 2,5</b>	<b>787 ± 156</b>	<b>1022 ± 240</b>
<b>20</b>	<b>167 ± 73</b>	<b>237 ± 88</b>	<b>5555 ± 2555</b>	<b>7042 ± 90</b>
21	191 ± 65	180 ± 26	>10000	>10000

<sup>a</sup> Concentration that produces 50% dissociation of the  $G\alpha_{i1}$  and  $G\alpha_{oA}$  subunits and recruitment of  $\beta$ -arrestin1 and 2, values represent the mean ± SEM of three determinations. Analogues in bold were tested for their impact to lower the mean arterial pressure in rats.

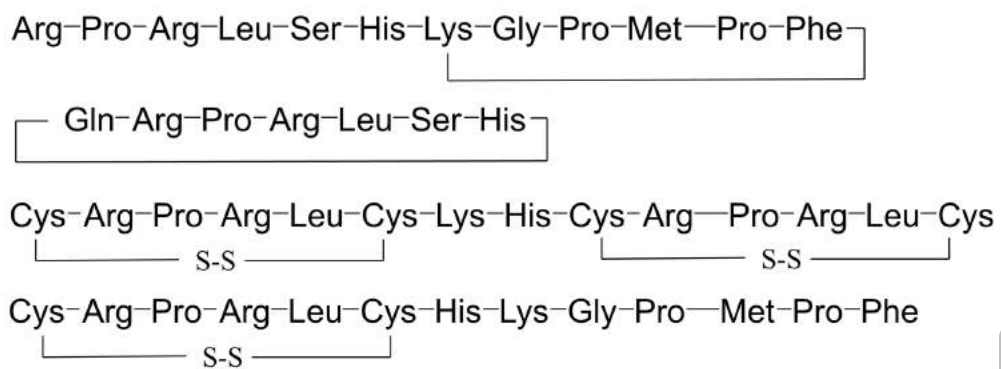


**Figure 1.** Amino acid sequences of selected macrocyclic derivatives of apelin-13.<sup>18,27,34,35</sup>

Accepted Manuscript

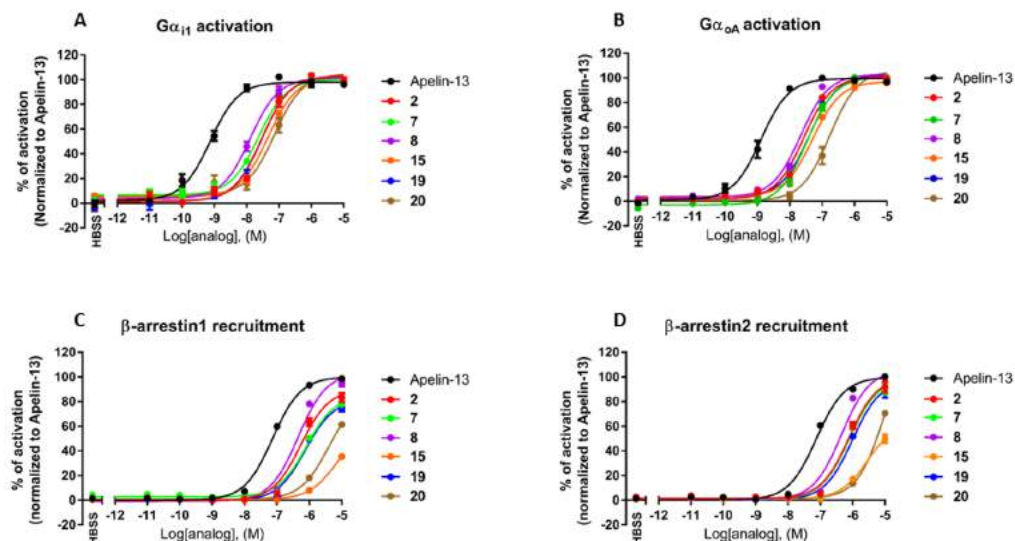


**Figure 2.** Functional activity of apelin-13 and a selection of macrocyclic analogues. Dose-response curves were determined using BRET-based assays, monitoring  $G\alpha_{i1}$  (A) and  $G\alpha_{oA}$  (B) activation and  $\beta$ -arrestin1 (C) and  $\beta$ -arrestin2 recruitment (D). Data are expressed as a percentage of apelin-13 maximal response. Data are the mean  $\pm$  SEM of three independent experiments performed in triplicate.

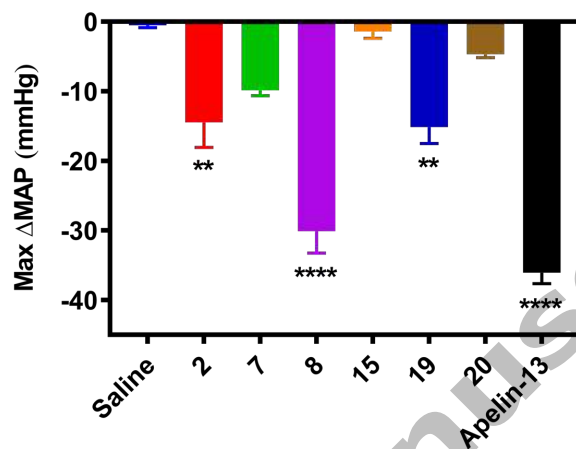


**Figure 3.** Maximal reduction of mean arterial pressure (Max  $\Delta$ MAP) induced by apelin-13 and a selection of macrocyclic analogues (19.6 nmol/kg i.v.) in anesthetized rats. Each bar represents the average value  $\pm$  SEM obtained with 5-16 animals. Statistical analyses were performed with a one-way ANOVA followed by a Dunnett's multiple comparisons test. \*  $<0.05$ , \*\*  $p < 0.005$  and \*\*\*\*  $p < 0.0001$  vs Saline.